Numerical Analysis of Flows in a Solar Chimney Power Plant with a Curved Junction

Tahar Tayebi*[1], Mahfoud Djezzar[2]

Energy Physics Laboratory, Department of Physics, Faculty of Exact Sciences, Constantine 1 University
Aïn El bey Road, Constantine, 25000, Algeria.

*[1]tahartayebi@gmail.com; [2]mdjezzar@yahoo.fr

Abstract

The Solar Chimney Power Plant System (SCPPS) is a simple solar thermal power plant that is capable of converting solar energy into thermal energy in the solar collector. In the second stage, the generated thermal energy is converted into kinetic energy in the chimney and ultimately into electric energy using a combination of a wind turbine and a generator. This study is to conduct a more detailed numerical analysis of solar chimney power plant system with a curved junction. This paper summarizes a numerical study flow in a solar chimney with a curved junction. The fluid is the air (Pr=0.702), and considered as a Newtonian and incompressible fluid. The governing equations are taken to be in the vorticity-stream function formulation in hyperbolic coordinates by using the Boussinesq approximation. For heating conditions, an isothermal walls of the collector has been supposed. Solution of the defined equations has been done with numerical control volume method. Additionally, the effect of the system geometry (the curved junction) on the heat transfer phenomenon in the solar chimney has been examined. Results are related to the temperature distribution and the velocity field in the chimney and in the collector.

Keywords

Solar Chimney Power Plant; Heat Transfer; Curved Junction; Hyperbolic Coordinates

Introduction

A Solar Chimney Power Plant System (SCPPS) is composed of a solar collector, to raise the energy level of the air by greenhouse effect of a chimney tower ensuring the circulation of air per gradient of density, and of an aero generator to produce electric power.

Professor Schlaich of Stuttgart originally proposed the solar chimney concept in the late 1970s (Schlaich, 1995). Less than 4 years after he presented this ides at a conference, construction on a pilot plant began in Manzanares, Spain, as a result of a joint venture between the German government and a Spanish utility. A 36 kW pilot plant was built, which produced electricity for 7 years, thus proving the efficiency and reliability of this novel technology. The chimney tower was 194.6m height, and the collector had a radius of 122m. Fundamental investigations for the Spanish system were reported by (Haaf, et al., 1983) in which a brief discussion of the energy balance, design criteria, and cost analysis was presented. Efforts were focused essentially on analyzing performances and cost of solar chimney. (Bernardes, et al., 1999) presented a theoretical analysis of a solar chimney, operating on natural laminar convection in steady state. In order to predict thermo-hydrodynamic behavior of air, temperature conditions were imposed on entrance, so as to guarantee steady laminar flow along the device. The mathematical model was analyzed by the method of Finite volumes in generalized coordinates. Velocity field and temperature distribution in the flow were obtained under imposed thermal conditions. (Von Backström & Fluri, 2006) investigated analytically the validity and applicability of the assumption that, for maximum fluid power, the optimum ratio of turbine pressure drop to pressure potential is 2/3. (Von Backström & Gannon, 2000) were interested mainly in a one-dimensional compressible flow for the thermodynamic variable as dependence on chimney height, wall friction, additional losses, internal drag and area exchange. (Pretorius & Kröger, 2006) evaluated the influence of a developed convective heat transfer equation, more accurate turbine inlet loss coefficient, quality collector roof glass and various types of soil on the performance of a large scale solar chimney power plant. (Ming, et al., 2006) presented a mathematical model to evaluate the relative static pressure and driving force of the solar chimney power plant system and verified the model with numerical simulations. (Maia et al.,2009) presented a theoretical analysis of a turbulent flow inside a solar chimney. They showed that the most important physical elements in a solar chimney system are the tower dimensions as they cause the most significant

variation in the flow behavior. An increase in the height and diameter of the tower produces the rise in the mass flow rate and decrement in the flow temperature. (Koonsrisuk & Chitsomboon, 2009) studied about the ventilation efficiency of solar chimney by comparing between five of the mathematical simulations and five of CFD simulation both from the previous researches. (Koonsrisuk & Chitsomboon, 2007) proposed dimensionless variables to guide the experimental study of flow in a small-scale solar chimney: a solar power plant to generate electricity. Computational fluid dynamics (CFD) methodology was employed to obtain results that are used to prove the similarity of the proposed dimensionless variables. (Pastohr et al., 2004) presented a numerical simulation result in which the storage layer was regarded as solid. In their paper, conjugate numerical simulations of the energy storage layer, the collector and the chimney have been conducted, and the characteristics of the heat storage system, and the flow and heat transfer in the whole system have been studied. (Zhou, et al., 2007) have performed an experimental study in a solar chimney. A pilot experimental solar chimney power setup consisting of an air collector of 10 m in diameter and an 8 m height chimney was built. The authors noted that the temperature difference between the collector outlet temperature and the one of the ambient usually might reach as much as 24.1 8 °C, which generates the driving force of the air flow in the setup. Their data analysis showed an air temperature inversion in the latter chimney after sunrise and this is due to the increase of solar radiation from the minimum. The phenomenon disappears once a driving force is generated by a temperature high enough to overcome it. (Koonsrisuk et al., 2010) described the constructal-theory search for the geometry of a solar chimney. (Sangi et al., 2011) developed a mathematical model to accurately describe the solar chimney power plant mechanism. Numerical profiles for the temperature, velocity and pressure in the collector of the solar chimney power plant were shown for three different solar radiations. (Chergui et al., 2010) presented a study considering the heat transfer process and the fluid flow in the collector and the chimney under some imposed operational conditions. The temperature difference through the Rayleigh number, the velocity field and the temperature distribution, through the system, have been evaluated. Results showed local flow characteristics and it appears that for most Rayleigh numbers, the flow seems laminar except for Raleigh number of 10^8 where there are some disturbances.

Problem Formulation and Basic Equations

A solar chimney has been taken into consideration which contains an incompressible fluid (air). The roof and ground surface create a vertical temperature gradient (active walls) (Fig.1).

The physical properties of the fluid are constant, apart from the density ϱ whose variations are at the origin of the natural convection. Viscous dissipation is neglected, just as the radiation (emissive properties of the two walls being neglected). It was accepted that the problem is bidimensionnal, permanent and laminar.

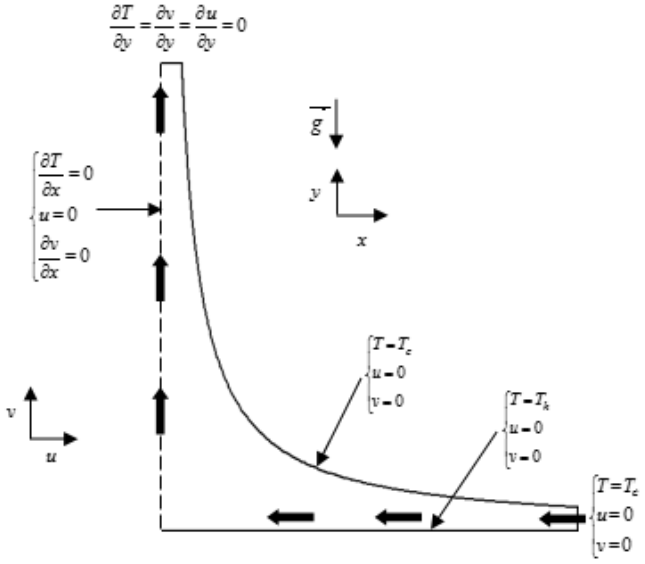

FIG. 1 PROBLEM STUDY AND BOUNDARY CONDITIONS

The laminar natural convection equations within the framework of the Boussinesq approximation are written:

- ***Continuity equation***

$$\frac{\partial u}{\partial x}+\frac{\partial v}{\partial y}=0 \tag{1}$$

- ***Vorticity equation***

$$u\frac{\partial \omega}{\partial x}+v\frac{\partial \omega}{\partial y}=\frac{\partial T}{\partial x}(g\beta)+\upsilon\left(\frac{\partial^2 \omega}{\partial x^2}+\frac{\partial^2 \omega}{\partial y^2}\right) \tag{2}$$

- ***Energy equation***

$$u\frac{\partial T}{\partial x}+v\frac{\partial T}{\partial y}=\frac{\lambda}{\rho Cp}\left(\frac{\partial^2 T}{\partial x^2}+\frac{\partial^2 T}{\partial y^2}\right) \tag{3}$$

It is convenient to define a reference frame such as the limits of the system result in constant values of the coordinates. The passage of the Cartesian coordinates

(x, y) to the hyperbolic coordinates (η, θ) is obtained by the following relations:

$$\left.\begin{aligned} x &= \sqrt{\frac{r+\eta}{2}} \\ y &= \sqrt{\frac{r-\eta}{2}} \end{aligned}\right\} \quad (4)$$

With:

$$r = \sqrt{\eta^2 + \theta^2} \quad (5)$$

Equations (1), (2) and (3) written then respectively:

$$\frac{\partial}{\partial \eta}\left(hV_\eta\right) + \frac{\partial}{\partial \theta}\left(hV_\theta\right) = 0 \quad (6)$$

$$V_\eta \frac{\partial T}{\partial \eta} + V_\theta \frac{\partial T}{\partial \theta} = \frac{1}{h}\frac{\lambda}{\rho Cp}\left(\frac{\partial^2 T}{\partial \eta^2} + \frac{\partial^2 T}{\partial \theta^2}\right) \quad (7)$$

$$\frac{V_\eta}{h}\frac{\partial \omega}{\partial \eta} + \frac{V_\theta}{h}\frac{\partial \omega}{\partial \theta} = \frac{\upsilon}{h^2}\left(\frac{\partial^2 \omega}{\partial \eta^2} + \frac{\partial^2 \omega}{\partial \theta^2}\right) + \frac{g\beta}{h}\left(\sqrt{\frac{r+\eta}{2r}}\frac{\partial T}{\partial \eta} + \sqrt{\frac{r-\eta}{2r}}\frac{\partial T}{\partial \theta}\right) \quad (8)$$

Where, h is the metric coefficient.

The equation for the stream function:

$$\omega = -\frac{1}{h^2}\left(\frac{\partial^2 \psi}{\partial \eta^2} + \frac{\partial^2 \psi}{\partial \theta^2}\right) \quad (9)$$

The quantities characteristic used for the dimensionless problem are the $\Delta T = T_h - T_c$ between The roof and ground surface, the metric coefficients in hyperbolic coordinates (h) as reference length and the thermal diffusivity of fluid α as characteristic velocity. The dimensionless mathematical model obtained is:

$$\omega^* = -\frac{1}{h^2}\left(\frac{\partial^2 \psi^*}{\partial \eta^2} + \frac{\partial^2 \psi^*}{\partial \theta^2}\right) \quad (10)$$

$$V_\eta{}^* \frac{\partial \omega^*}{\partial \eta} + V_\theta{}^* \frac{\partial \omega^*}{\partial \theta} = \frac{\Pr}{H}\left(\frac{\partial^2 \omega^*}{\partial \eta^2} + \frac{\partial^2 \omega^*}{\partial \theta^2}\right) + Ra\,\Pr\left(\sqrt{\frac{r+\eta}{2r}}\frac{\partial T^*}{\partial \eta} + \sqrt{\frac{r-\eta}{2r}}\frac{\partial T^*}{\partial \theta}\right) \quad (11)$$

$$V_\eta{}^* \frac{\partial T^*}{\partial \eta} + V_\theta{}^* \frac{\partial T^*}{\partial \theta} = \frac{1}{H}\frac{\lambda}{\rho Cp}\left(\frac{\partial^2 T^*}{\partial \eta^2} + \frac{\partial^2 T^*}{\partial \theta^2}\right) \quad (12)$$

Where:

$$V_\eta{}^* = \frac{1}{H}\frac{\partial \psi^*}{\partial \theta}; V_\theta{}^* = -\frac{1}{H}\frac{\partial \psi^*}{\partial \eta} \quad (13)$$

The boundary conditions are the following ones:

- ***The roof of the collector***

$$V_\eta{}^* = V_\theta{}^* = \frac{\partial \psi^*}{\partial \theta} = \frac{\partial \psi^*}{\partial \eta} = 0 \text{ and } T^* = 0 \quad (14)$$

- ***The axis of symmetry***

$$\frac{\partial V_\eta{}^*}{\partial \theta} = \frac{\partial^2 \psi^*}{\partial \theta^2} = 0, V_\theta{}^* = \frac{\partial \psi^*}{\partial \eta} = 0, \frac{\partial T^*}{\partial \theta} = 0 \quad (15)$$

- ***The ground***

$$V_\eta{}^* = V_\theta{}^* = \frac{\partial \psi^*}{\partial \theta} = \frac{\partial \psi^*}{\partial \eta} = 0 \text{ and } T^* = 1 \quad (16)$$

- ***Collector inlet***

$$V_\eta{}^* = V_\theta{}^* = \frac{\partial \psi^*}{\partial \theta} = \frac{\partial \psi^*}{\partial \eta} = 0 \text{ and } T^* = 0 \quad (17)$$

- ***Chimney outlet***

$$\frac{\partial V_\eta{}^*}{\partial \eta} = \frac{\partial^2 \psi^*}{\partial \eta \partial \theta} = 0, \frac{\partial V_\theta{}^*}{\partial \eta} = \frac{\partial^2 \psi^*}{\partial \eta^2} = 0 \text{ and } \frac{\partial T^*}{\partial \theta} = \quad (18)$$

Numerical Method

To solve this system of equations with associated boundary conditions equations, a numerical solution by the method of finite volumes has been taken into account, presented by (Patankar, 1980) using a numerical code (computer programme).The power law scheme was used for the discretization. The iterative method used for the numerical solution of algebraic system of equations (Matrix) is the Gauss-Seidel, with an under-relaxation process. The following condition is used to declare convergence:

$$\left|\frac{\max T^{n+1} - \max T^n}{\max T^{n+1}}\right| \leq 10^{-6} \quad (19)$$

Where: ***n+1*** is the current iteration and ***n*** is the previous iteration.

Fig. 2 shows the physical domain and the computational domain.

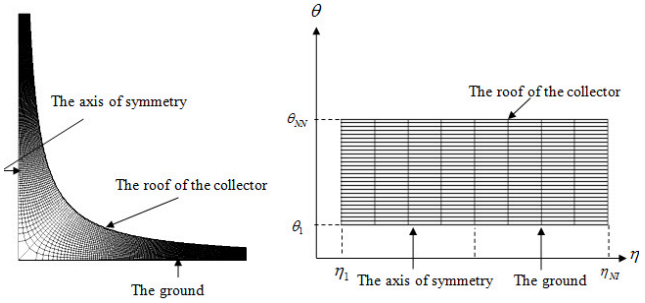

FIG. 2 PHYSICAL DOMAIN AND COMPUTATIONAL DOMAIN

Results and Discussion

The grid dependence has been investigated using different mesh sizes before settling to a mesh size of (350 x 22).

Our objective is to analyze the effect of geometry on heat transfer and flow of air into the chimney. For this reason, we presented the isotherms and isovelocity lines in two different geometries for three different Rayleigh numbers.

For the validation of the computational problem, our results were compared with those of literature: (Sangi et al., 2011), and the study of (Pastohr et al., 2004) and (Chergui et al., 2010).

Figs. 3–5 show the dimensionless isothermal lines for the first geometry and for Rayleigh numbers equal to

10^3, 10^4 and 10^5 respectively. When the Rayleigh number is small, as being lower or equal to 10^4, the heat transfer is essentially conductive, so the isotherms have the same form as the walls and the maximum temperature is located near the ground in the collector due to heat transfer exchange between this surface and the airflow beneath the cover. For a Rayleigh number equal to 10^5 swirls in isothermal lines are also observed in the collector area.

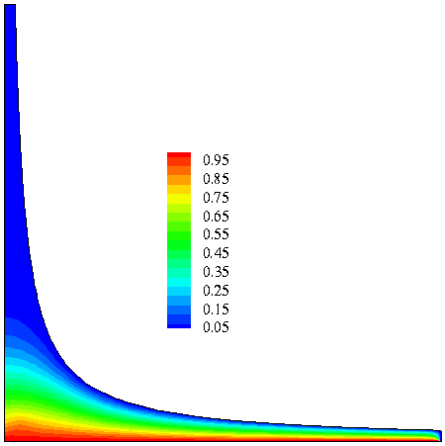

FIG. 3 ISOTHERMAL LINES FOR THE FIRST GEOMETRY AND Ra=10^3

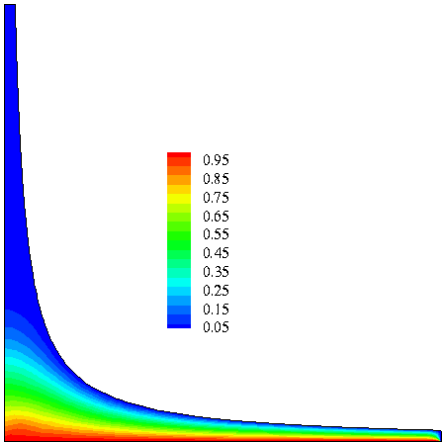

FIG. 4 ISOTHERMAL LINES FOR THE FIRST GEOMETRY AND Ra=10^4

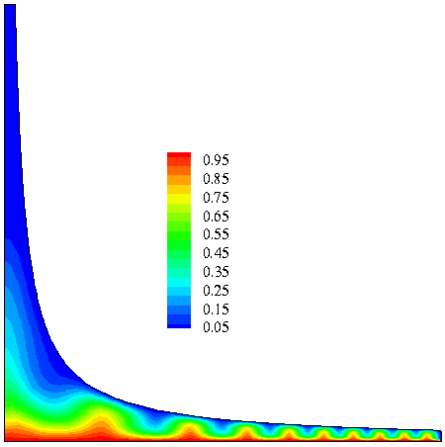

FIG. 5 ISOTHERMAL LINES FOR THE FIRST GEOMETRY AND Ra=10^5

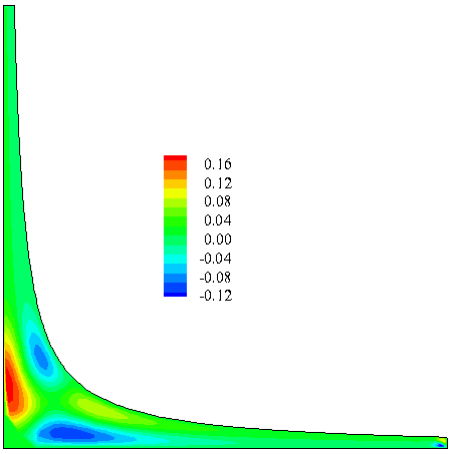

FIG. 6 ISOVELOCITY LINES FOR THE FIRST GEOMETRY AND Ra=10^3

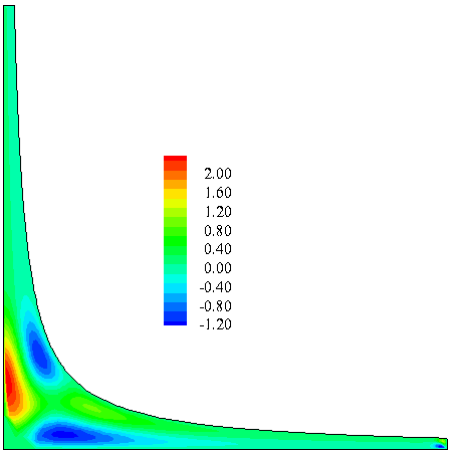

FIG. 7 ISOVELOCITY LINES FOR THE FIRST GEOMETRY AND Ra=10^4

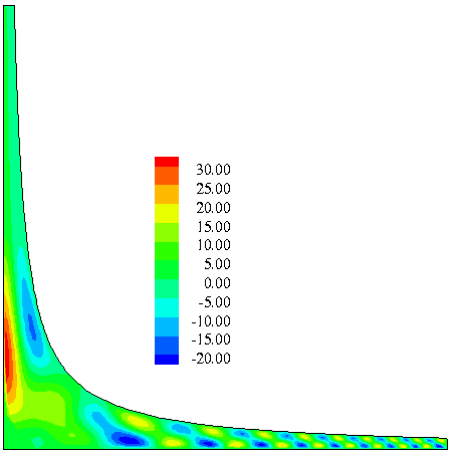

FIG. 8 ISOVELOCITY LINES FOR THE FIRST GEOMETRY AND Ra=10^5

Figs. 6–8 represent the isovelocity lines for the first geometry and different Rayleigh number values. For Ra = 10^3 and 10^4, the velocity magnitude increases with the rise of the Rayleigh number and its maximum value is located approximately at the inlet of the chimney as it is reported in literature (Pastohr et al., 2004), (Sangi et al., 2011) and (Chergui et al., 2010). For these Rayleigh numbers, isovelocity lines are smooth

characterizing a laminar flow, along the chimney and the collector, except for the region of curved junction and the inlet of the collector where different zones of flow recirculation can be observed due to instability of airflow in these areas. For Ra = 10^5 an instability (different zones of flow recirculation) of airflow along the collector can be observed. The isovelocity lines values show an appreciable increase in the flow. This means that the transfer is done primarily by convection and predominates on the conduction.

When the distance between the ground and the roof is increased (second geometry), a disturbance of isothermal lines can be observed in the collector zone at the beginning of a Rayleigh number equal to 10^4 (Figs. 9–11) and the natural convection is dominant.

Figs. 12–14 illustrate the dimensionless velocity lines for second geometry and for Rayleigh 10^3,10^4 and 10^5 respectively. It should be noted that its value is higher than the one calculated in the first geometry and always its maximum is located at the inlet of the chimney. A large zone of flow recirculation is inverted located below the curved wall.

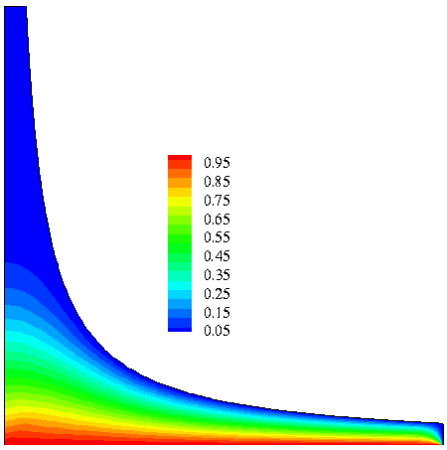

FIG. 9 ISOTHERMAL LINES FOR THE SECOND GEOMETRY AND Ra=10^3

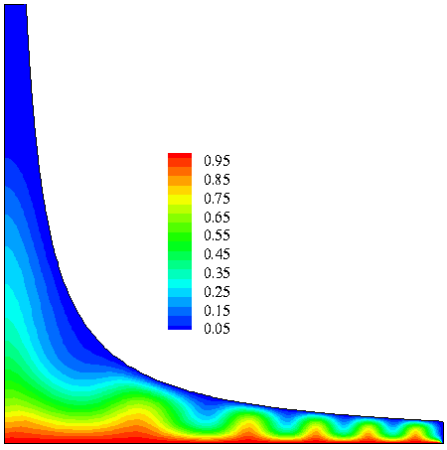

FIG. 10 ISOTHERMAL LINES FOR THE FIRST GEOMETRY AND Ra=10^4

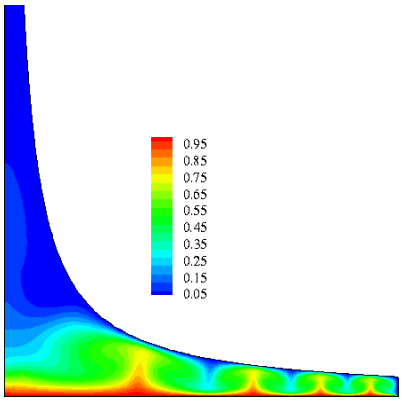

FIG. 11 ISOTHERMAL LINES FOR THE FIRST GEOMETRY AND Ra=10^5

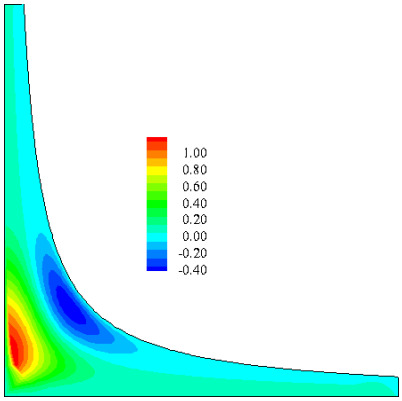

FIG. 12 ISOVELOCITY LINES FOR THE SECOND GEOMETRY AND Ra=10^3

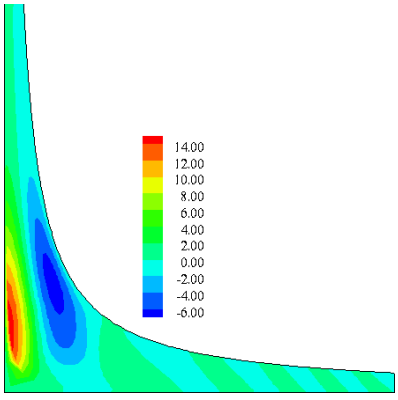

FIG. 13 ISOVELOCITY LINES FOR THE SECOND GEOMETRY AND Ra=10^4

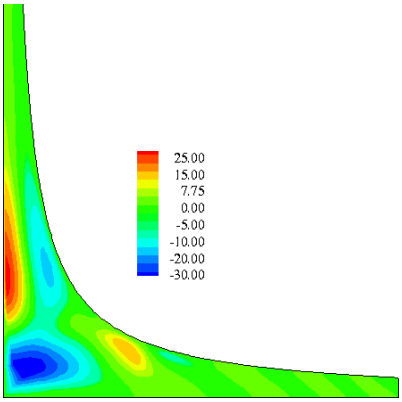

FIG. 14 ISOVELOCITY LINES FOR THE SECOND GEOMETRY AND Ra=10^5

Fig. 15 shows the air velocity profile through the collector for the two geometries considered and Rayleigh 10^3. The velocity increases through the collector by decreasing the radius, but it increases more sharply by reaching the chimney base. When the collector radius is constant, an increase of distance between the ground and the roof (second geometry) causes an increase of the air velocity. The same results are observed in literatures by (Pastohr et al., 2004), (Sangi et al., 2011) and (Chergui et al., 2010).

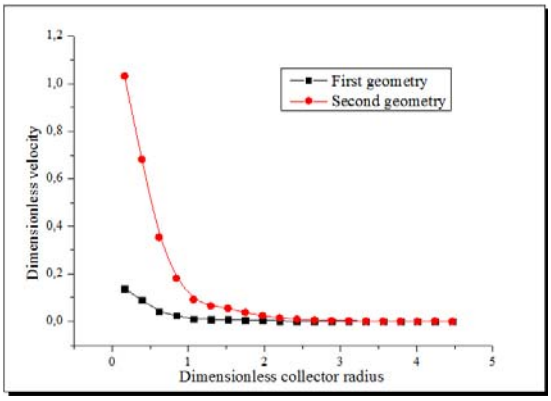

FIG. 15 VELOCITY PROFILE THROUGH THE COLLECTOR FOR THE TWO GEOMETRIES CONSIDERED AND Ra=10^3

Conclusions

In this paper a thermo-hydrodynamic analysis for air motion in natural convection, laminar flow and steady state has been presented for a solar chimney with prescribed boundary conditions. A validated computer program was adapted to the solar chimney configuration to solve the governing equations, using the method of finite volumes. Meanwhile, the effect of the system geometry with a curved junction on the heat transfer process and the fluid flow in the system has been investigated, along with two different geometries considered. The simulations were executed based on three values of the Rayleigh number: Ra=10^3, Ra=10^4 and Ra=10^5.

Results showed that the maximum velocities are gotten at the inlet of the chimney tower and and its values were increased by increasing the difference between ground and roof of the collector for all Rayleigh numbers.

This result will help the solar chimney designer correctly locate the turbine in the solar chimney power plant.

Nomenclature

Symbols

C_p: Specific heat at constant pressure, J kg^{-1} K^{-1};

h: Metric coefficient, m;

H: Dimensionless metric coefficient;

P_r: Prandtl number;

Ra: Rayleigh number;

T: Fluid's temperature, K;

T_h: Temperature of the ground, K;

T_c: Temperature of the roof, K;

ΔT: $T_h - T_c$, K;

u , v: Velocities components according to coordinates x and y, m s^{-1};

V_η, V_θ: Velocities components according to coordinates η and θ, m s^{-1};

x, y: Cartesian coordinates, m;

Greek Symbols

β: Thermal expansion coefficient, K^{-1};

λ: Thermal conductivity, W.m^{-1} K^{-1};

υ: Kinematic viscosity, m^2 s^{-1};

ρ: Density, kg.m^{-3};

η,θ: Hyperbolic coordinates;

ψ: Stream function, m^2 s^{-1};

ω: Vorticity ,s^{-1};

Subscripts

h : Hot;

c: Cold;

$*$: Dimensionless parameters.

REFERENCES

Bernardes, M. A. d. S., Molina Valle, R., Cortez, M. F. B. Numerical analysis of natural laminar convection in a radial solar heater, International Journal of Thermal Science 38 (1999) 42-50.

Chergui, T., Larbi, S., Bouhdjar, A. Thermo-hydrodynamic aspect analysis of flows in solar chimney power plants—A case study. Renewable and Sustainable Energy Reviews 14 (2010) 1410–1418.

Haaf, W., Friedrich, K., Mayr, G., Schlaich, J. Solar chimneys, Part I: principle and construction of the pilot plant in Manzanares, International Journal of Solar Energy 2 (1983) 3–20.

Koonsrisuk, A., Chitsomboon, T. Dynamic similarity in solar chimney modeling. Solar Energy 81 (12)(2007) 1439-1446.

Koonsrisuk, A., Chitsomboon, T. Accuracy of theoretical

models in the prediction of solar chimney performance. Solar Energy 83(2009) 1764-1771.

Koonsrisuk, A., Lorente, S., Bejan, A.. Constructal solar chimney configuration. International Journal of Heat and Mass Transfer (2010) 53:327–333.

Maia, C.B., Ferreira, A.G., Valle, R.M., Cortez, M.F.B. Theoretical evaluation of the influence of geometric parameters and materials on the behavior of the air flow in a solar chimney, Computers and Fluids. 38 (2009) 625-636.

Ming, T.Z., Liu, W., Xu, G.L., Fan, A.W. A study of the solar chimney power plant systems. Journal of Engineering Thermodynamics. 3 (2006) 505-517.

Schlaich, J. The Solar Chimney: Electricity from the Sun, Edition Axel Menges, Stuttgart, Germany, 1995.

Patankar, S.V. Numerical heat transfer and fluid flow, Hemisphere, Washington, D.C, 1980.

Pastohr, H., Kornadt, O., Gurlebeck, K. Numerical and analytical calculations of the temperature and flow field in the upwind power plant, International Journal of Energy Research. 28 (2004) 495-510.

Pretorius, J.P., Kröger, D.G. Critical evaluation of solar chimney power plant performance, Solar Energy 80 (2006) 535–544.

Sangi, R., Amidpour, M., Hosseinizadeh, B. Modeling and numerical simulation of solar chimney power plants, Solar Energy 85 (2011) 829–838

Von Backstrom, T.W., Cannon, A.J. Compressible flow through solar power plant chimneys, Journal of Solar Energy Engineering 122 (2000) 138–145.

Von Backström, T.W., Fluri, T.P. Maximum fluid power condition in solar chimney power plants-an analytical approach, Solar Energy 80 (2006) 1417-1423.

Zhou, X., Yang, J., Xiao, B., Hou, G. Hou, Experimental study of temperature field in a solar chimney power setup, Applied Thermal Engineering. 27 (2007) 2044-2050.